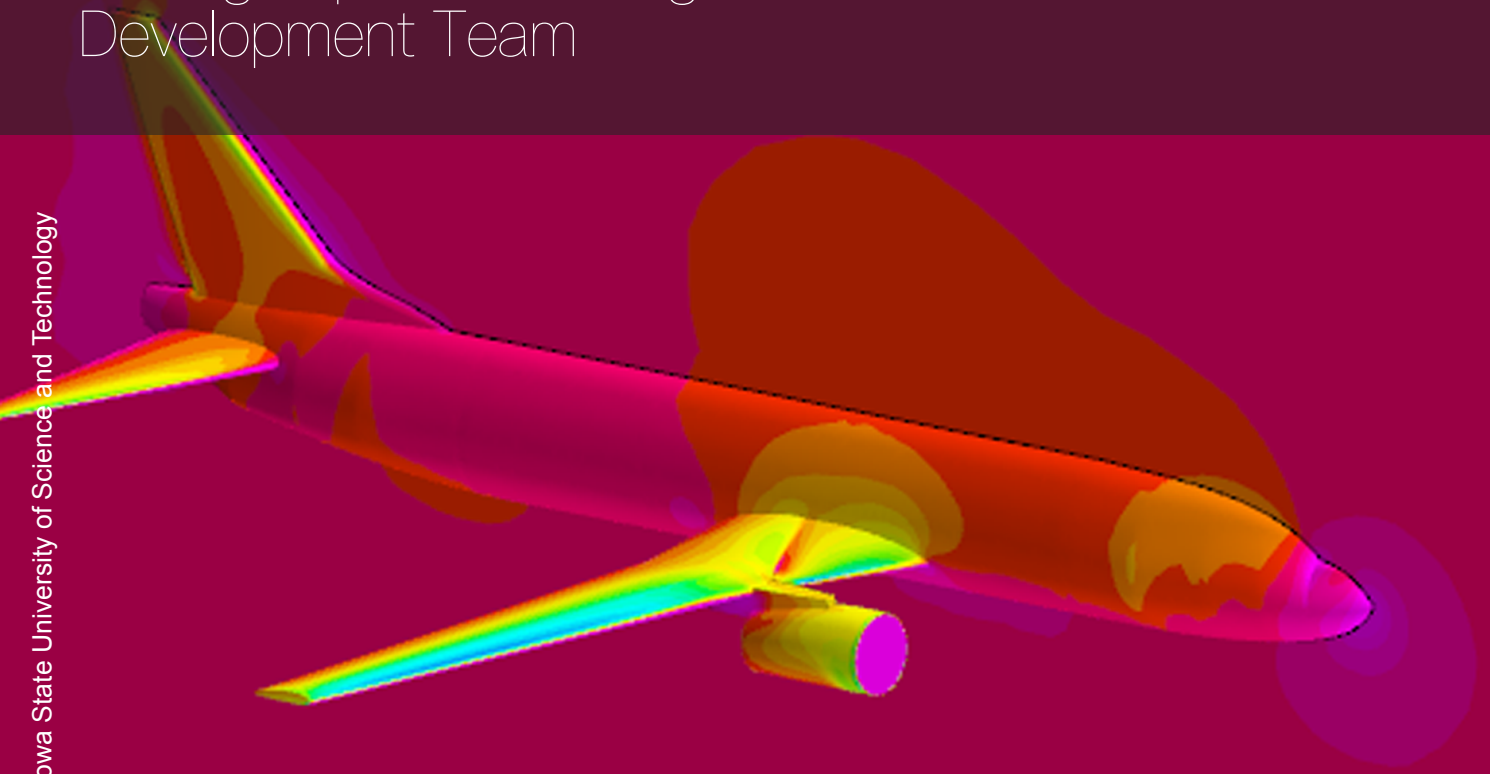


BEF Analysis Report

Star-CCM+ Analysis of Airfoils
October 31, 2022

Boeing Experimental Flight
Development Team



Iowa State University of Science and Technology

IOWA STATE
UNIVERSITY

BEF Analysis Report

Star-CCM+ Analysis of Airfoils October 31, 2022

by

Boeing Experimental Flight
Development Team

Project Members

Jacob Carlson
Tyler Chandler
Ayan Asim
Khanh Hoang
Dominic Lim
Ryan Rouleau

Instructor: Matthew Nelson, Christine Nelson, and Peter Sherman
Industry Advisors: Ryan Engel and Rohan Sharma
Teaching Assistant: Cole Drenth
Project Duration: August, 2022 - December, 2022

Cover: Static Pressure Scalar of the AL-37 Aircraft

**IOWA STATE
UNIVERSITY**

Abstract

The objective of this team is to create and test a new set of truss-braced wings. Flight data from the AL-37 remote control aircraft and Computational Fluid Dynamics (CFD) data can be used to lead into this design. The next step is to determine an airfoil for the new designs. The goal of this study is to determine an optimal airfoil for the scale of our aircraft that has sufficient lift and static stability data using CFD testing. Once a new airfoil is selected, it can be used to design and construct a new truss-braced wing to test in comparison to a Boeing 737 MAX 8-like wing. A model was constructed in SolidWorks of the AL-37, and imported into Star-CCM. CFD tests were done for a selection of airfoils and compared to the AL-37's CFD and flight data. Of the tested airfoils, the NACA 3510 was chosen due to having sufficient lift and static stability data.

Contents

Abstract	i
Symbols	v
1 Introduction	1
1.1 Overall	1
1.2 About the AL-37	1
1.3 About the Truss-Braced Wings	2
2 Methodology	3
2.1 Physical Model Data	3
2.2 Design Parameters	3
2.3 CAD	4
2.3.1 XFLR5	4
2.4 Star-CCM+	4
2.5 CFD Data Excel Sheet	5
2.5.1 Lift-to-Drag Ratio vs. Angle of Attack	5
2.5.2 Center of Gravity and Neutral Point	6
3 Data Analysis	7
3.1 Acquisition	7
3.2 Control Variable Data	7
3.3 Airfoil Analysis	10
3.3.1 NACA-2412	10
3.3.2 YS-930	11
3.3.3 NACA 1412	12
3.3.4 NACA 2211	13
3.3.5 NACA 3510	15
3.3.6 NACA 4413	16
3.3.7 NACA 6410	19
3.3.8 Clark Y	20
4 Results	21
5 Conclusion	26
6 Bibliography	27
A Data Graphing Utility Source Code	28
B Post-CFD MATLAB Analysis Code	30

List of Figures

1.1	AL-37 Approaching Landing	1
1.2	First iteration of the Truss-Braced Wing	2
2.1	AL-37 CAD Model	4
3.1	CL vs. AoA with AL-37 Wing	7
3.2	CD vs. AoA with AL-37 Wing	7
3.3	CM vs. AoA with AL-37 Wing	8
3.4	L/D vs. AoA with AL-37 Wing	8
3.5	Optimized Linear Range with AL-37 Wing	8
3.6	CG and NP Placement with AL-37 Wing	9
3.7	L/D vs. AoA with NACA 2412 Wing	10
3.8	Optimized Linear Range with NACA 2412 Wing	10
3.9	CG and NP Placement with NACA 2412 Wing	10
3.10	L/D vs. AoA with YS-930 Wing	11
3.11	Optimized Linear Range with YS-930 Wing	11
3.12	CG and NP Placement with YS-930 Wing	11
3.13	L/D vs. AoA with NACA 1412 Wing	12
3.14	Optimized Linear Range with NACA 1412 Wing	12
3.15	CG and NP Placement with NACA 1412 Wing	12
3.16	CL vs. AoA with NACA 2211 Wing	13
3.17	CD vs. AoA with NACA 2211 Wing	13
3.18	CM vs. AoA with NACA 2211 Wing	13
3.19	L/D vs. AoA with NACA 2211 Wing	14
3.20	Optimized Linear Range with NACA 2211 Wing	14
3.21	CG and NP Placement with NACA 2211 Wing	14
3.22	L/D vs. AoA with NACA 3510 Wing	15
3.23	Optimized Linear Range with NACA 3510 Wing	15
3.24	CG and NP Placement with NACA 3510 Wing	15
3.25	L/D vs. AoA with NACA 4413 Wing	16
3.26	Optimized Linear Range with NACA 4413 Wing	16
3.27	CG and NP Placement with NACA 4413 Wing	16
3.28	NACA 4413 Preliminary Analysis via XFLR5	17
3.29	NACA 4413 Lift Results	17
3.30	NACA 4413 Coefficient of Lift Results	18
3.31	NACA 4413 Pitching Moment at Low Angles of Attack	18
3.32	NACA 4413 Pitching Moment at High Angles of Attack	18
3.33	L/D vs. AoA with NACA 6410 Wing	19
3.34	Optimized Linear Range with NACA 6410 Wing	19
3.35	CG and NP Placement with NACA 6410 Wing	19
3.36	L/D vs. AoA with Clark Y Wing	20
3.37	Optimized Linear Range with Clark Y Wing	20
3.38	CG and NP Placement with Clark Y Wing	20
4.1	AoA vs. Lift for All Candidate Airfoils	21
4.2	AoA vs. Drag for All Candidate Airfoils	22
4.3	AoA vs. Pitching Moment for All Candidate Airfoils	22
4.4	AoA vs. L/D for All Candidate Airfoils	23
4.5	Optimized Linear Range for All Candidate Airfoils	23

List of Tables

4.1	Candidate Airfoil CFD Data	25
4.2	Eliminated Airfoil CFD Data	25

Symbols

AoA = angle of attack

c = mean chord length

C_D = coefficient of drag

C_L = coefficient of lift

C_M = coefficient of moment

c_{root} = root chord

c_{tip} = tip chord

CG = center of gravity

D = drag

F_A = axial force

F_N = normal force

L = lift

l_{wing} = length from the root to the wing tip

L/D = lift-to-drag ratio

M_y = pitching moment

$M_{y,np}$ = pitching moment at the neutral point

NP = neutral point

P_∞ = static pressure of the freestream

q_∞ = dynamic pressure of the freestream

R = gas constant

S = planform area

$S_{fuselage\ section}$ = area of the fuselage under the wing

S_{wing} = area of a single wing from the root to the tip

T_∞ = temperature of the freestream

U_{∞} = velocity of the freestream

w_{fuselage} = width of the fuselage

x_{cg} = x position of the center of gravity

x_{np} = x position of the neutral point

x_{ref} = reference x position

α = angle of attack

ρ_{∞} = fluid density of the freestream

1

Introduction

1.1. Overall

The Boeing Experimental Flight Project is a group in the Make to Innovate program at Iowa State University. The project's main objective is to develop and test new parts for an electric aircraft. Previous semesters involved developing new wings and testing them using a wind tunnel. This semester, we are determining a new airfoil to use for future wing configurations and analyzing them via Computational Fluid Dynamics analysis.

1.2. About the AL-37



Figure 1.1: AL-37 Approaching Landing

The AL-37 is a remote control aircraft from Freewing. It is a 1/19 scale of the Boeing 737 MAX 8. It is 78.74 inches (in) long and has a wingspan of 72.04 in. It is powered by two 6S 2952-2100Kv inrunner motors with 12-blade electronic ducted fans. It also features a fully operational LED lighting system and retractable landing gear, like an actual Boeing 737 MAX 8. The project's version of the AL-37 has some modified electronics. These include a Pixhawk 4 Flight Controller system to track and record data for the aircraft. The wiring was also modified to allow for the Pixhawk controller to eventually take automated control over the aircraft.

1.3. About the Truss-Braced Wings



Figure 1.2: First iteration of the Truss-Braced Wing

The initial iteration of the truss-braced wings were constructed at roughly 1/17 scale to the Boeing 737-800. It is 72 in long and has a wingspan of 78.36 in. The wings are constructed out of blue foam laid up with carbon fiber. Both the wing and the truss structures utilize the S1223 airfoil, resulting in high lift at certain angles of attack. However, the airfoil was discovered to be problematic at angles of attack exceeding 5 degrees, making it a potentially unstable airfoil for climbing and take-off procedures. It was determined that the team should utilize a different airfoil as a result of this discovery.

2

Methodology

2.1. Physical Model Data

The AL-37's Pixhawk 4 Flight Controller is capable of collecting performance data during test flights. This allows us to further optimize the CAD model and Star-CCM+ parameters to accurately compare data. The following table lists flight parameters gathered from these test flights.

Average Indicated Air Speed	54.5 mph
Average Flight Altitude	260 ft
Maximum Flight Altitude	359 ft

For determining a physical representation of center of gravity, the aircraft was outfitted with its battery and balanced on top of a PVC pipe, the nose being perpendicular to the pipe's axial axis. Members moved the aircraft forward and backward until the aircraft nose and tail were stable and not tipping over. This placed the CG as slightly behind the nacelle, which matches information from the manufacturer.

2.2. Design Parameters

Because of the unique design of the AL-37 base model wings, the team is trying to select a new airfoil for the truss-braced wing design while keeping the fuselage and empennage constant. However, the trailing edge of the AL-37 base model has two sections that are angled back together instead of having one straight edge. In order to decrease complexity, the team determined keep a consistent aspect ratio to maintain a similar induced drag. Based on the dimensions of the AL-37 base model, we kept the planform area the same at 475.25 in² and the wing span as 62.88 in. We also kept a constant wing tip chord at 3.75 in and are varying the root chord to match the correct wing area and aspect ratio. Below are the equations to find the root chord dimension.

S is the planform area, $S_{fuselage\ section}$ is the area of the fuselage under the wing, S_{wing} is the area of a single wing from the root to the tip, c_{root} is the root chord, c_{tip} is the tip chord, $w_{fuselage}$ is the width of the fuselage, and l_{wing} is the length from the root to the wing tip.

$$S = S_{fuselage\ section} + 2S_{wing}$$
$$S = (w_{fuselage}c_{root}) + 2(l_{wing} \frac{c_{root} + c_{tip}}{2})$$
$$c_{root} = \frac{S - l_{wing}c_{tip}}{w_{fuselage} + l_{wing}}$$

With the width of the fuselage at 7.78 in and the length of the wing at 27.55 in, the necessary root chord to produce the same area and aspect ratio as the AL-37 base model is 10.53 in.

Planform Area	475.25 in ²
Wing Span	62.88 in
Length of Wing	27.55 in
Root Chord	10.53 in
Tip Chord	3.75 in

2.3. CAD

The CAD development process began by creating a model of the current AL-37 Aircraft. The model was developed by taking accurate measurements of the physical components with a dial caliper, paired with images to ensure the shape was correct. The initial design was composed of three separate SolidWorks parts: the fuselage/empennage, the wings, and the engine. After the individual parts were complete, an assembly was formed for the entire aircraft. With the original AL-37 model finalized, Star-CCM+ analysis began in order to obtain control performance coefficients. The development of the original AL-37 CAD model was crucial as all future wing designs would be based off the fuselage and empennage of the original design to ensure consistency.

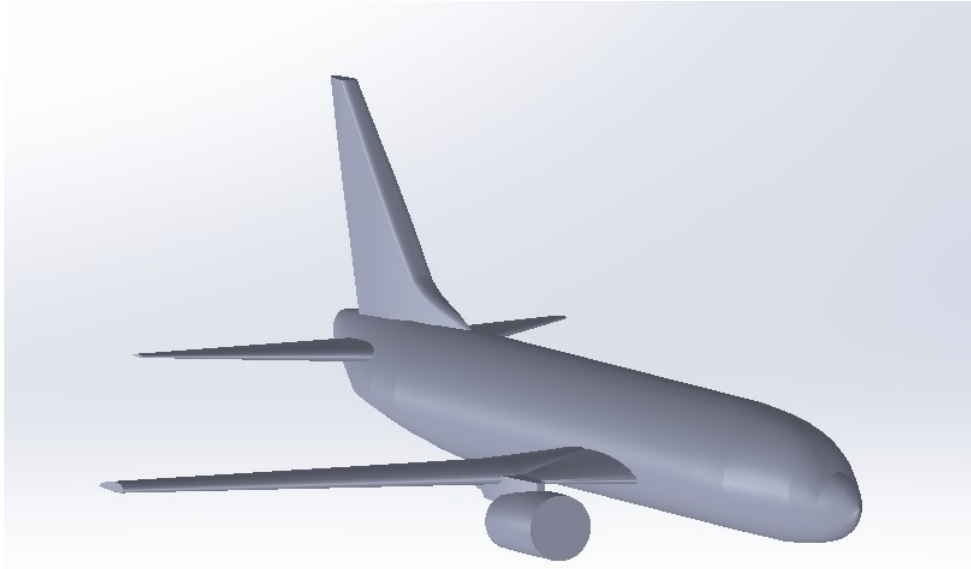


Figure 2.1: AL-37 CAD Model

The next step in our CAD development was to create new wings with consistent dimensions but different airfoils. The goal of this was to identify an airfoil that would optimize the L/D of the AL-37 model while still maintaining stability through an angle of attack range of -4 degrees to 8 degrees. The root chord, root tip, and wing span dimensions were all set to 10.53 in, 3.75 in, and 27.55 in respectively. Then using airfoil databases such as airfoiltools.com and XFLR5, the coordinates of each airfoil were imported and scaled in order to make the wings. The final step in the CAD development was assembling the new wing to the original AL-37 fuselage.

2.3.1. XFLR5

XFLR5 is an airfoil analysis program that our team used to identify preliminary airfoils after some basic research on airfoiltools.com. From previous test flights, our Reynolds number was known, thus accurate analysis could be performed to identify the L/D optimization for our flight conditions but not the stability. From the XFLR5 analysis, the team was able to narrow the search down to various airfoils that were ultimately tested in Star-CCM+ and discussed in this report.

2.4. Star-CCM+

Star-CCM+ is a Computational Fluid Dynamic software that was utilized in order to obtain theoretical aircraft performance values for both the original AL-37 model and subsequent wing designs. Unfortunately, no wind tunnels available at Iowa State University are large enough to hold our aircraft, and it would require scaling down the wings a significant amount, which would create more error. Star-CCM+ is an extensive program, thus our team sought out the expertise of Professor Travis Grager of Iowa

State University. With his help, our team was able to set specific air pocket parameters in Star-CCM+ to test our SolidWorks models.

The process for integrating the SolidWorks assemblies into Star-CCM+ began by saving the assembly as a single parasolid body. This parasolid was then imported into the air pocket designed in Star-CCM+. The next step was to select and name all of the faces according to specific parameters in order for a mesh to be developed. After generating a mesh of the parasolid body, the entire aircraft was subtracted from the air pocket. The simulation was then ready to be ran, however it was too complex for a local server to run in a reasonable time, thus computers in the High Performance Cluster at Iowa State University was used.

After the simulation was completed, numerous scalar plots were available in order to qualitatively identify the aerodynamic performance of the aircraft such as pressure distribution, streamlines, and dynamic viscosity.

(Insert a Scalar Image in lab).

Along with the scalar scenes, quantitative data such as the normal force, axial force, and moment along the wing is calculated for an angle of attack range of -5 to 10 degrees. This data is then used to calculate the specific aerodynamic coefficients of the aircraft.

(Insert Image of Every 1000 Plot)

2.5. CFD Data Excel Sheet

Professor Travis Grager created Microsoft Excel sheets that assist in analyzing the CFD data from Star-CCM+. These Excel sheets can produce multiple aerodynamic performance plots based on the given inputs and the CFD data. However, we will focus on the lift-to-drag vs. angle of attack plot and the center of gravity and neutral point plot for this report.

2.5.1. Lift-to-Drag Ratio vs. Angle of Attack

By inputting the altitude used the Star-CCM+ simulation, the total pressure and temperature can be interpolated and imported from standard atmospheric tables. With the total pressure and temperature, the air density can be found using the following equation.

$$P_{\infty} = \rho_{\infty} R T_{\infty}$$

Using the density and the inputted velocity for Star-CCM+, the dynamic pressure can be calculated with the following equation.

$$q_{\infty} = \frac{1}{2} \rho_{\infty} U_{\infty}^2$$

The Star CCM+ simulation provided the normal force and axial force on a half-body aircraft at a certain angle of attack. These forces will need to be doubled to account for a full-body aircraft, but the variables will allow us to find the lift and drag at the angles of attack with the following equations.

$$L = 2(F_N \cos(\alpha) - F_A \sin(\alpha))$$

$$D = 2(F_N \sin(\alpha) + F_A \cos(\alpha))$$

Since we have the lift and drag, the coefficient of lift and the coefficient of drag at each angle of attack can be calculated with dynamic pressure and the planform area in these equations.

$$C_L = \frac{L}{q_{\infty} S}$$

$$C_D = \frac{D}{q_{\infty} S}$$

Finally, the lift-to-drag ratio at each angle of attack would be the quotient of the coefficient of lift over the coefficient of drag.

$$L/D = \frac{C_L}{C_D}$$

The lift-to-drag ratios are then plotted against the angles of attack, and these graphs will be compared to the AL-37 base model for each airfoil.

2.5.2. Center of Gravity and Neutral Point

In order to calculate the neutral point, we can set up a moment equation using static equilibrium for the normal force from a reference point.

$$M_y = -(x_{np} - x_{ref})F_N + M_{y,np}$$

We can take the partial derivative of the moment equation by angle of attack. By definition, the partial derivative of the moment at the neutral point in terms of angle of attack has to be zero. We can also use the rate of change from our pitching moment and normal force data since they were iterated over angle of attack. Therefore, the Excel sheet finds the optimal linear range for the pitching moment and normal force and provides us the slope.

$$\frac{\partial M_y}{\partial \alpha} = -(x_{np} - x_{ref}) \frac{\partial F_N}{\partial \alpha} + 0$$

We can rearrange the previous equation to finally get the location of the neutral point. In addition, the center of gravity has already been found using physical methods as mentioned earlier in the report.

$$x_{np} = x_{ref} - \frac{\frac{\partial M_y}{\partial \alpha}}{\frac{\partial F_N}{\partial \alpha}}$$

The static margin of the aircraft can be found using the neutral point, the center of gravity, and the mean chord length. We are aiming for a static margin of 5% to 25% in order to be stable with some maneuverability.

$$(x_{np} - x_{cg})/c$$

Obtaining the neutral point and center of gravity is useful for determining the aircraft's stability since having neutral point behind the center of gravity is statically stable. The Excel sheet plots the neutral point and center of gravity in terms of the aircraft's length. The stability of the aircraft can also be quantified by the static margin. The plot and static margin of each airfoil will then be compared to the AL-37 base model.

3

Data Analysis

3.1. Acquisition

Inputs such as airspeed (mph) and altitude (ft) were entered into the Star-CCM+ files for each wing. Data was gathered by running the Star-CCM+ files through the campus High-Performance Cluster with a batch script. The results were exported into a CSV file and copied into Professor Grager's Excel template. The inputs and coordinates of the aircraft weight were inserted to output the necessary tables and graphs.

3.2. Control Variable Data

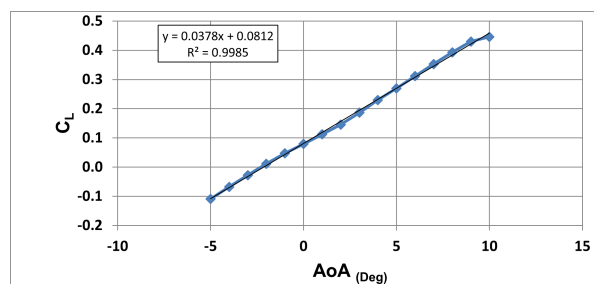


Figure 3.1: CL vs. AoA with AL-37 Wing

The coefficient of lift is shown to be 0.0790 at 0 degrees angle of attack, or at steady-level flight. The corresponding value for lift is 1.93 lbf at steady-level, with a maximum value of 10.8 lbf at 10 degrees.

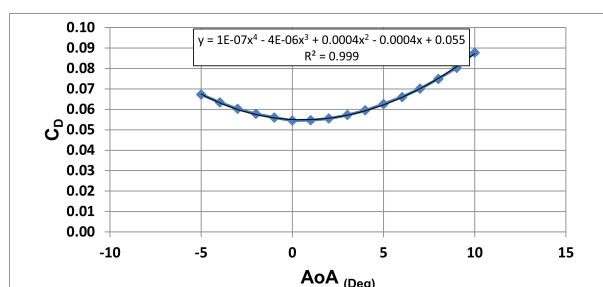


Figure 3.2: CD vs. AoA with AL-37 Wing

The coefficient of drag is 0.0545 at steady-level flight. Drag is calculated as 1.32 at steady-level flight, and 2.14 at 10 degrees angle of attack.

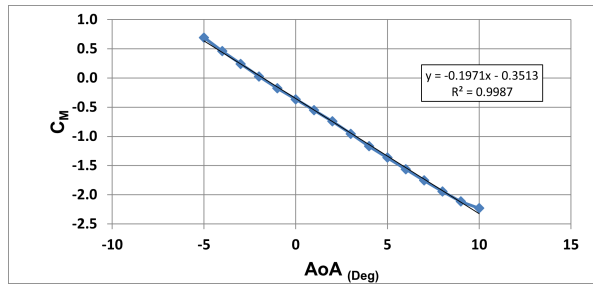


Figure 3.3: CM vs. AoA with AL-37 Wing

The coefficient of moment is shown as a downward curve, with the point of 0 moment being at roughly -2 degrees. Therefore at steady-level flight, there is a negative moment being generated.

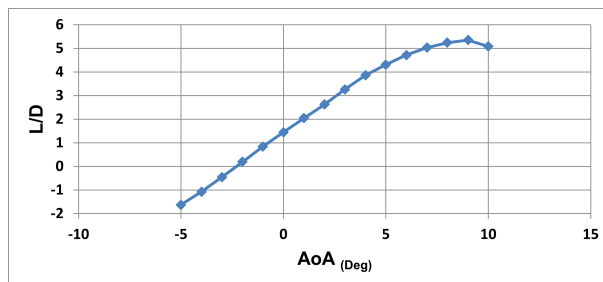


Figure 3.4: L/D vs. AoA with AL-37 Wing

The value of lift-over-drag, is maximized at roughly 9 degrees angle of attack, with a value of 5.09. The curve starts to drop after 10 degrees, implying angles larger than 10 degrees will cause the aircraft to approach stalling conditions. At steady-level flight, the L/D is 1.45, meaning it generating more lift than drag at 0 degrees.

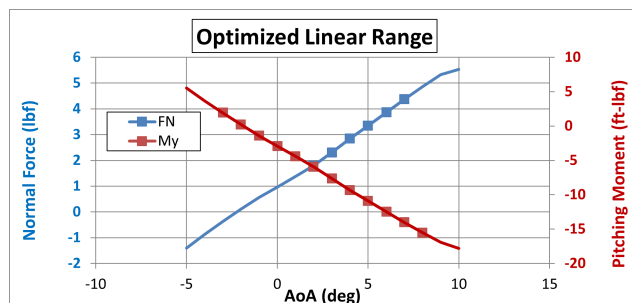


Figure 3.5: Optimized Linear Range with AL-37 Wing

The optimized angle of attack of the aircraft is calculated by finding where the normal force and pitching moment intersect. For the control AL-37 Wing, the optimized linear range provides an angle of attack of 2 degrees.

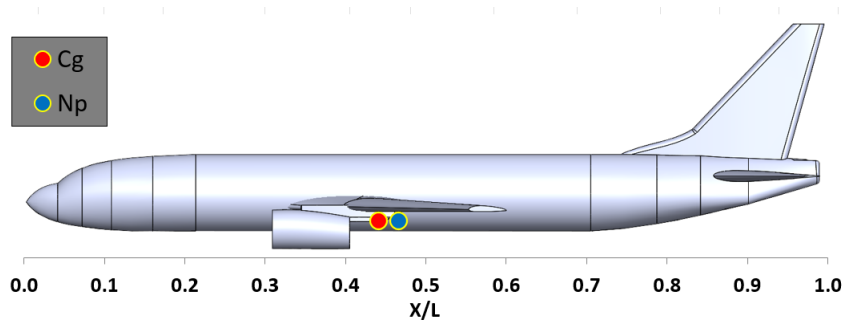


Figure 3.6: CG and NP Placement with AL-37 Wing

The placement of the neutral point in relation to the center of gravity. The neutral point is placed behind the center gravity, 46.6% from the nose tip into the fuselage, or 3.08 ft. This gives a positive static margin of 25.17%, which means the aircraft is stable with the AL-37 wing. The targeted static margin value for the selected airfoils is between 5 and 25%.

The center of gravity placement is near identical to what was physically measured, being just behind the nacelle of the aircraft with batteries loaded. This means that our model is accurate to a point.

3.3. Airfoil Analysis

Eight airfoils were selected based on initial graphs from airfoiltools.com, XFLR5, or from recommendations from advisors: the NACA airfoils 1412 [3], 2211, 2412 [4], 3510, 4413, and 6410; the YS-930 [5]; and the Clark-Y [6]. CAD models of each wing were created and put under analyses.

3.3.1. NACA-2412

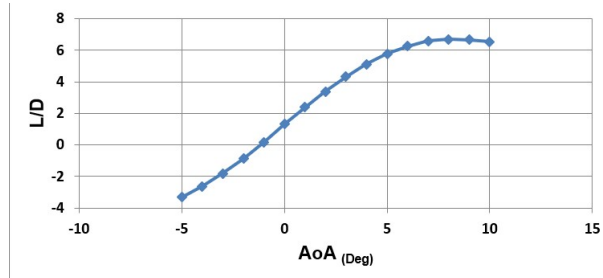


Figure 3.7: L/D vs. AoA with NACA 2412 Wing

The NACA 2412 was the first airfoil we tested. It has a maximum L/D at 8 degrees angle of attack, roughly 6.3. The L/D at steady-level flight is around 1.3, a downgrade to the AL-37's L/D values.

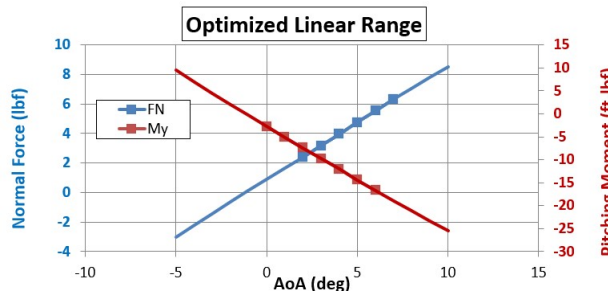


Figure 3.8: Optimized Linear Range with NACA 2412 Wing

The optimized linear range for the NACA 2412 provides roughly 3 degrees angle of attack, with a normal force of around 2 lbf and pitching moment of roughly -10 lbf-ft.

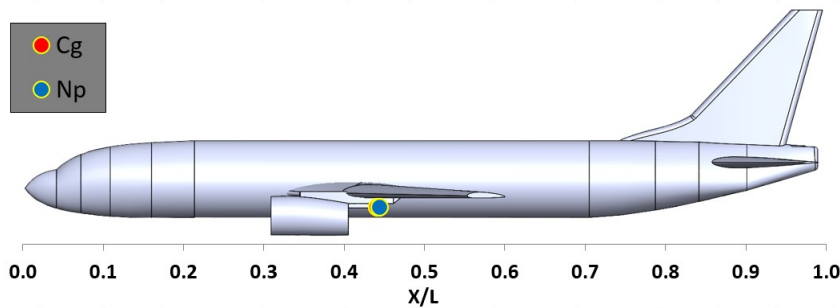


Figure 3.9: CG and NP Placement with NACA 2412 Wing

The CG is placed nearly on top of the NP, with a static margin of 3.71%. This makes the aircraft stable, albeit barely.

3.3.2. YS-930

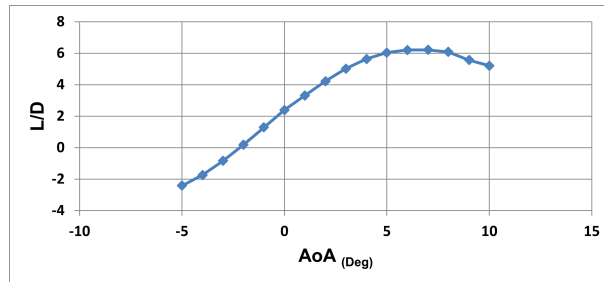


Figure 3.10: L/D vs. AoA with YS-930 Wing

The YS-930 has a maximum L/D ratio of roughly 6.1 lbf at 7 degrees angle of attack. At steady-level flight, the L/D is 2.2.

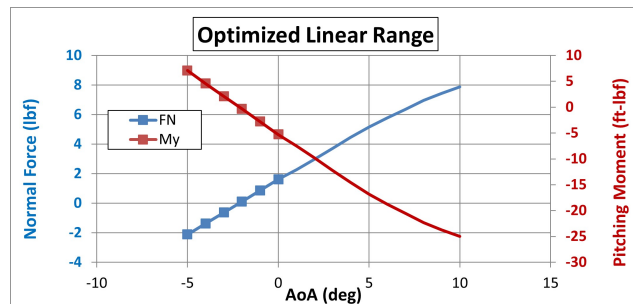


Figure 3.11: Optimized Linear Range with YS-930 Wing

The optimized linear range, like the NACA 2412, provides roughly 3 degrees angle of attack, with a slightly higher normal force of 3 lbf and similar pitching moment.

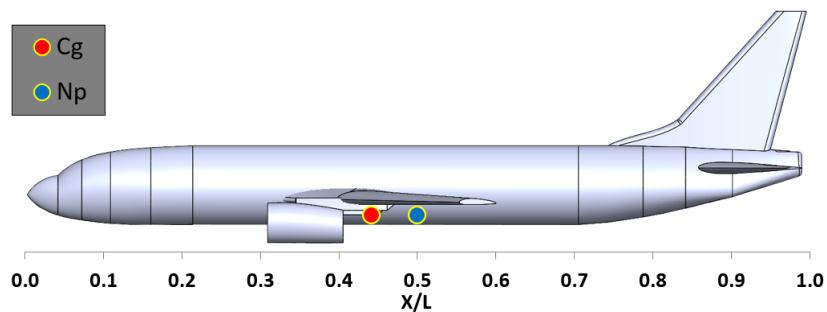


Figure 3.12: CG and NP Placement with YS-930 Wing

The center of gravity is further in front of the neutral point compared to the AL-37 airfoil, with a static margin of 58%. This puts it above our desired range for static margin, but the aircraft is very stable.

3.3.3. NACA 1412

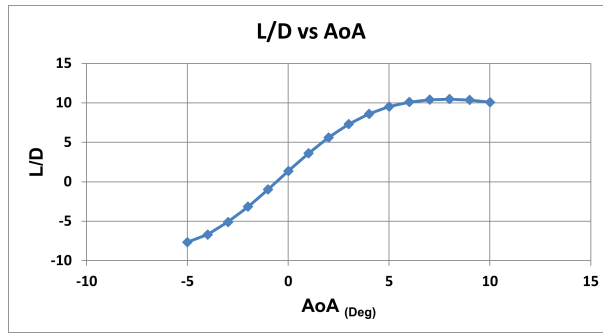


Figure 3.13: L/D vs. AoA with NACA 1412 Wing

The maximum lift-to-drag ratio is 10.48 at 8 degrees, which is higher than the AL-37 base model of 9.87 at 7 degrees. However, the lift-to-drag ratio at 0 degrees is 1.35 for the NACA 1412 assembly and is lower than 4.22 for the AL-37 base model.

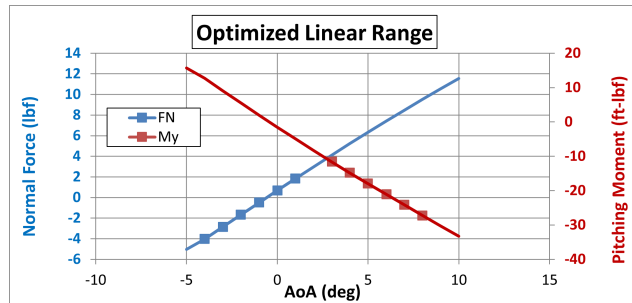


Figure 3.14: Optimized Linear Range with NACA 1412 Wing

The linear range of the normal force in terms of the angle of attack for the NACA 1412 assembly is from -5 lbf to 12 lbf and has a slope of 1.17 lbf/degrees. Meanwhile, the AL-37 base model's linear range is from -3 lbf to 11 lbf with a slope of 0.93 lbf/degrees. The NACA 1412 assembly has a pitching moment in terms of the angle of attack linear range of 16 lbf-ft to -34 lbf-ft and a slope of -3.12 lbf-ft/degrees. The AL-37 base model is from 10 lbf-ft to -33 lbf-ft and has a slope of -3.11 lbf-ft/degrees.

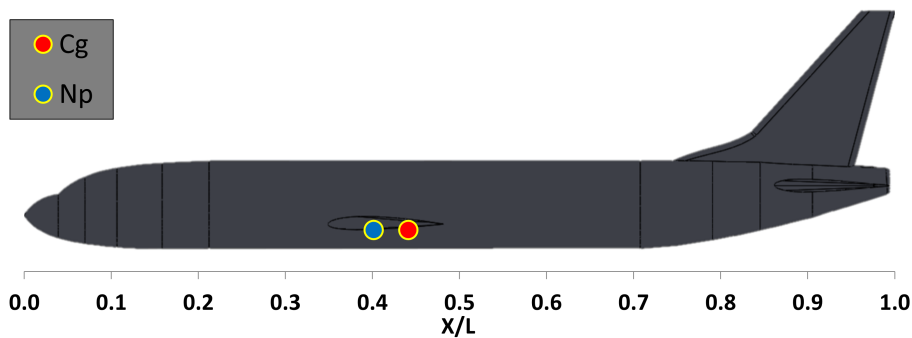


Figure 3.15: CG and NP Placement with NACA 1412 Wing

The center of gravity is 35 in from the nose or at 0.44 of the total length. The neutral point of the NACA 1412 assembly, also from the nose, is 32 in or at 0.40 of the length. Therefore, the NACA 1412 assembly is unstable due to the neutral point being ahead of the center of gravity with a static margin of -40%. Meanwhile, the AL-37 base model has a static margin of 25% and is stable.

3.3.4. NACA 2211

The following graphs were generated from the aforementioned Excel spreadsheet.

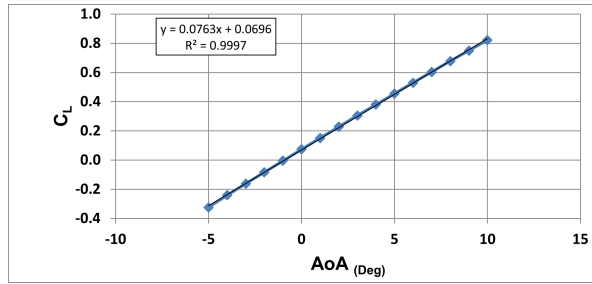


Figure 3.16: CL vs. AoA with NACA 2211 Wing

The coefficient of lift is shown to be 0.0737 at 0 degrees angle of attack, or at steady-level flight. The corresponding value for Lift is 1.80 lbf at steady-level, with a maximum value of 20.0 lbf at 10 degrees.

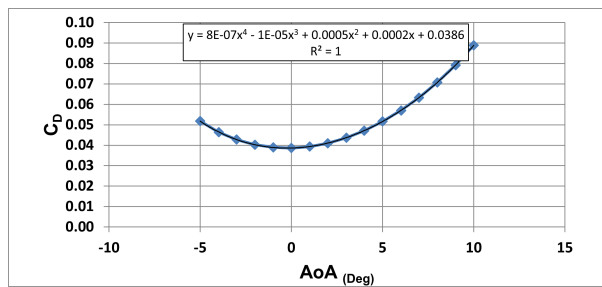


Figure 3.17: CD vs. AoA with NACA 2211 Wing

The coefficient of drag is 0.0387 at steady-level flight. Drag is calculated as 0.9418 at steady-level flight, and 2.1653 at 10 degrees angle of attack.

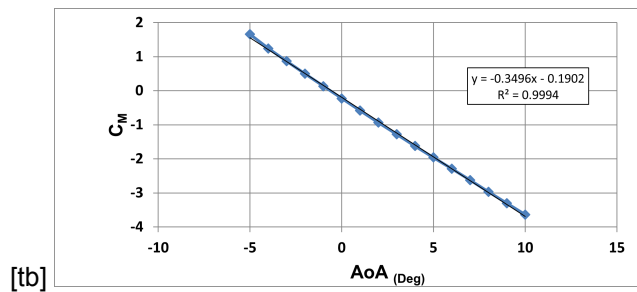


Figure 3.18: CM vs. AoA with NACA 2211 Wing

The coefficient of moment is shown as a downward curve, with the point of 0 moment being at roughly -1 degrees. Therefore at steady-level flight, there is a negative moment being generated.

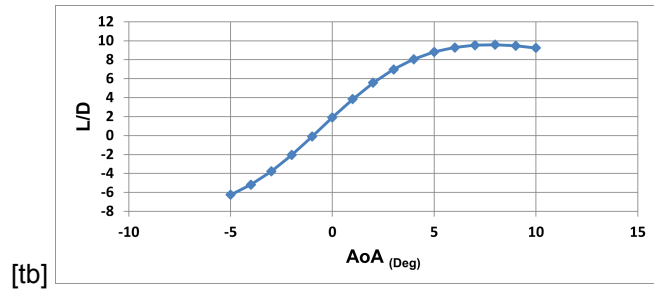


Figure 3.19: L/D vs. AoA with NACA 2211 Wing

The value of lift-over-drag, is maximized at roughly 8 degrees angle of attack, with a value of 9.59. The curve starts to drop after 10 degrees, implying angles larger than 10 degrees will cause the aircraft to approach stalling conditions. At steady-level flight, the L/D is 1.91, meaning it generating more lift than drag at 0 degrees.

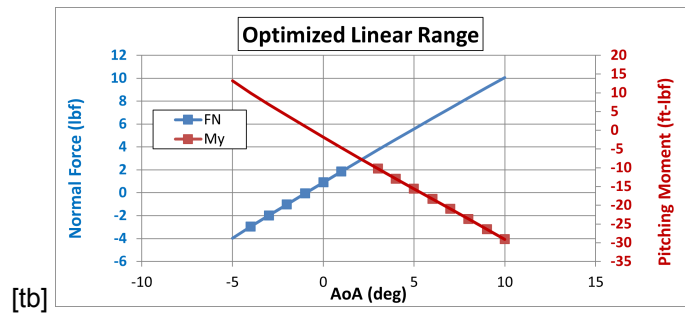


Figure 3.20: Optimized Linear Range with NACA 2211 Wing

In the optimized linear range of the NACA 2211, the ideal angle in regards to both value is roughly 3 degrees, where the lines intersect. At that point, Fn is equal to 3 lbf and My is roughly -7.5 lbf-ft.

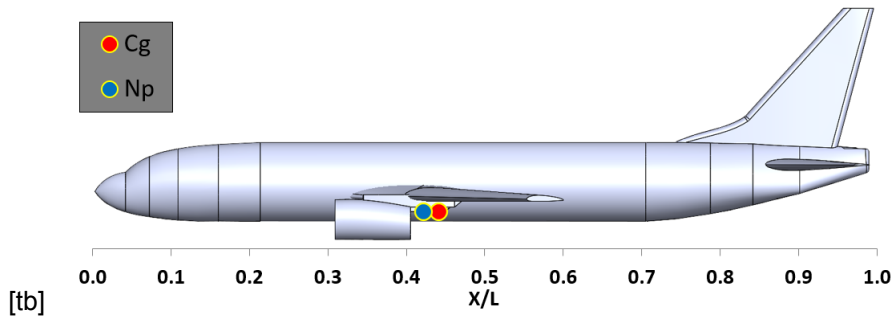


Figure 3.21: CG and NP Placement with NACA 2211 Wing

The placement of the neutral point in relation to the center of gravity. The neutral point is placed in front of the center gravity, 42.2% from the nose tip into the fuselage, or 2.79 ft. This gives a negative static margin, which means the aircraft is unstable with the NACA 2211 wing.

3.3.5. NACA 3510

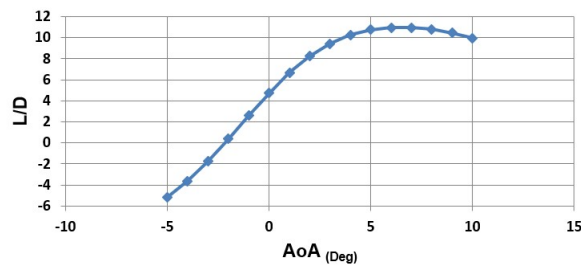


Figure 3.22: L/D vs. AoA with NACA 3510 Wing

The max L/D of the AL-37 with the NACA 3510 wing is 10.965 at an angle of attack of 6 degrees. From the airfoils tested, this is the second highest L/D values falling just short of the Clark Y. It is also important to note that over a range of alpha 0 degrees to 5 degrees the NACA 3510 also has the second highest L/D falling just short of the Clark Y once again.

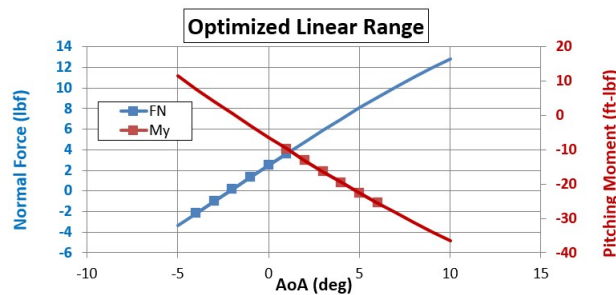


Figure 3.23: Optimized Linear Range with NACA 3510 Wing

The optimized angle of attack of the aircraft is calculated by finding the where the normal force and pitching moment intersect. For the NACA 3510 the optimized angle of attack is 1 degree.

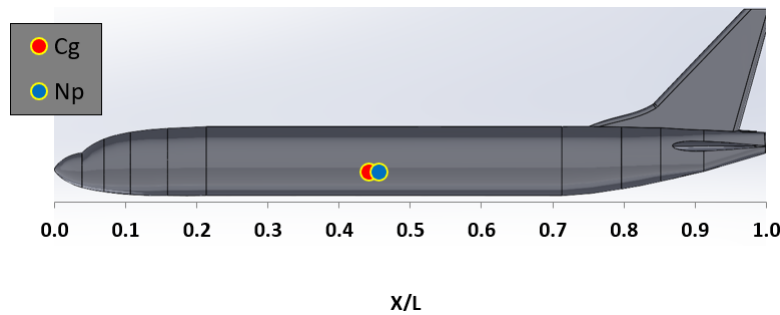


Figure 3.24: CG and NP Placement with NACA 3510 Wing

The relationship between the center of gravity and the neutral point of the aircraft is extremely important in order to define the stability. The center of gravity of the aircraft is 2.917 ft from the nose while the neutral point is 3.006 ft from the nose. This leads to a static margin of 13.69%.

3.3.6. NACA 4413

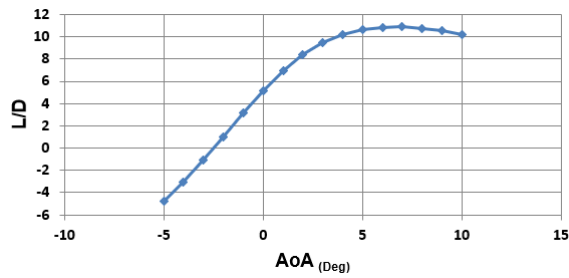


Figure 3.25: L/D vs. AoA with NACA 4413 Wing

As shown in figure, the NACA 4413 on the AL-37 has demonstrated the max L/D at roughly angle of attack of 7 degrees at 10.8785, just close to the results obtained just after the NACA 3510. Based on this data, we are able to see a lower stall angle past the peak of angle of attack 7 degrees, losing its lift fairly slowly as the NACA 4413 was designed to perform under slow speed conditions.

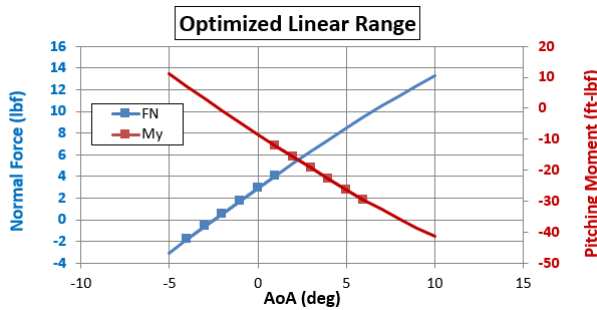


Figure 3.26: Optimized Linear Range with NACA 4413 Wing

For the NACA 4413 in the optimized linear range, we are able to see that the ideal angle of attack falls roughly at 2 degrees, where the blue and red lines intersect, pointing towards a normal force of 5.19 lbf and pitching moment of -15.88 lbf-ft.

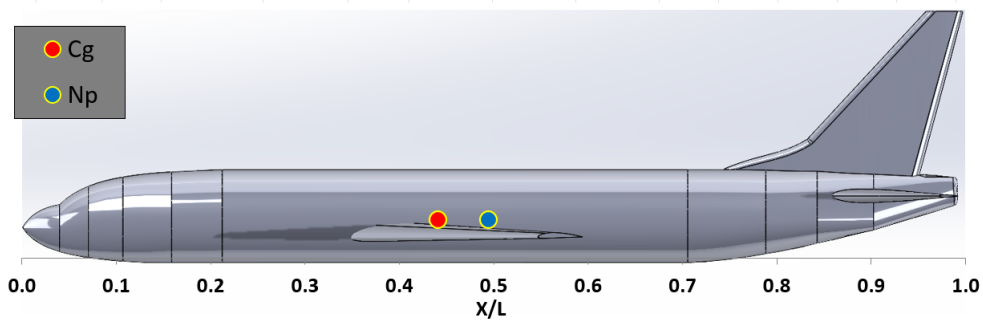


Figure 3.27: CG and NP Placement with NACA 4413 Wing

As we are able to see from the model assembly, the neutral point and the center of gravity is relatively close to each other at 2.9 ft and 2.94 ft from the nose of the AL-37 based on the NACA 4413 airfoil. With this, we were able to achieve a positive static margin of 53.97%.

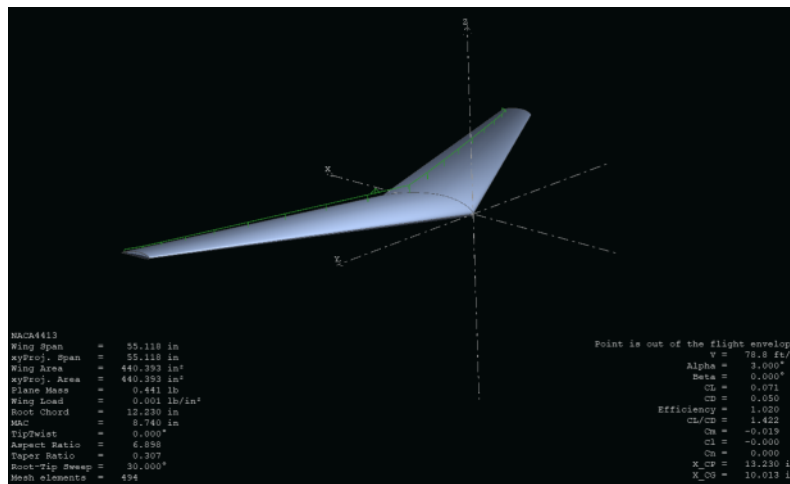


Figure 3.28: NACA 4413 Preliminary Analysis via XFLR5

Due to Solidworks modeling issues early in the development process, preliminary analysis of the NACA 4413 airfoil was conducted by creating the model and running through base testing on XFLR5 with the given wing and flight parameters. The AL-37 aircraft is given cruise speed of Mach=0.07 (roughly 100kmh or 60mph), the coefficient of lift distribution demonstrates low lift forces upon cruise angle of attack and has only demonstrated lift beyond angle of attack at 4 degrees. As representation of the NACA 4413 airfoil, it is a good representation of a low-speed airfoil used for low-speed flight, however the representation of low-speed flight is with relation to actual aircraft that would cruise at Mach=0.3 to Mach=0.6 (within the incompressible to subsonic region) before transitioning towards the transonic region of flight. As recommendation, the NACA-4413 airfoil would need to compensate with a wider wing span as well as a higher cruise flight velocity to achieve a higher lift coefficient distribution.

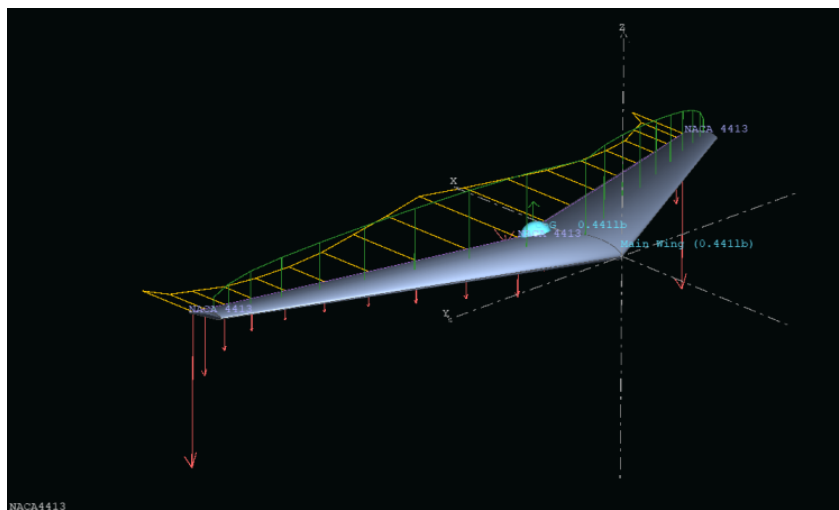


Figure 3.29: NACA 4413 Lift Results

Preliminary results has concluded that the NACA 4413 airfoil produces up to no lift, or close to zero coefficient of lift up to angle of attack at 3 degrees, represented as the cruising angle of attack for most aircraft including the AL-37. This is due to the relatively high camber of the NACA 4413 airfoil that would require a longer chord line as well needed a wider wing span to compensate for the flow over the surfaces of the airfoil as it cruises at low-speed/low-Mach speeds. As we can see from the simulation image above, the airfoil is represented at nearly angle of attack of 9 degrees to 10 degrees and would be relatively close to the pre-stall point for most aircraft.

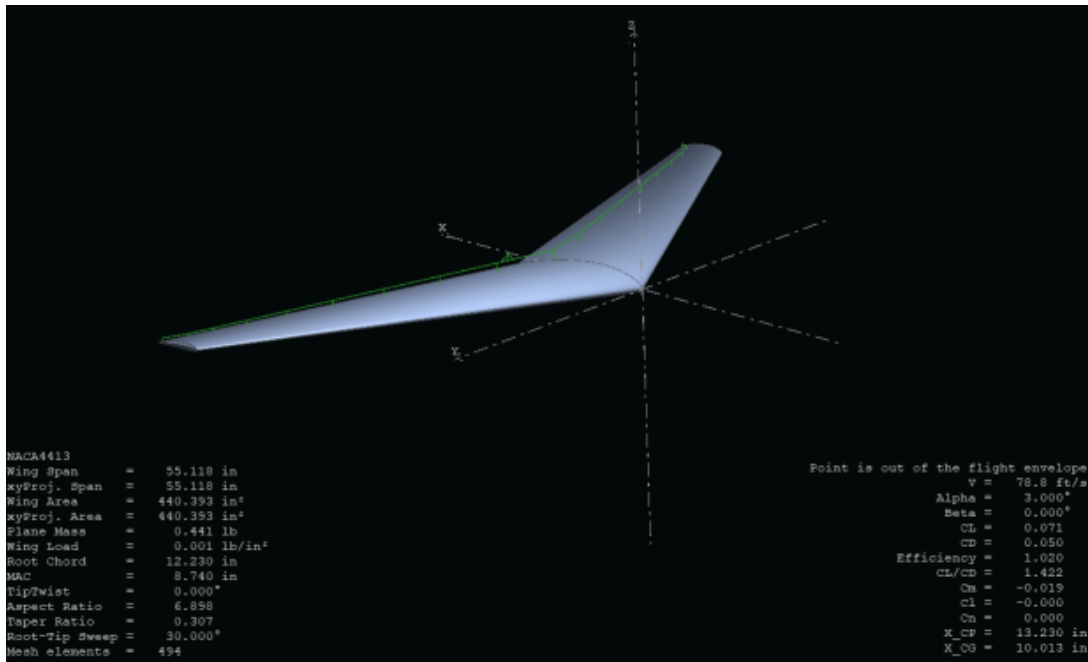


Figure 3.30: NACA 4413 Coefficient of Lift Results

The NACA 4413 represented as the image provided at angle of attack at 3 degrees with coefficient of lift demonstrated at CL=0.071.

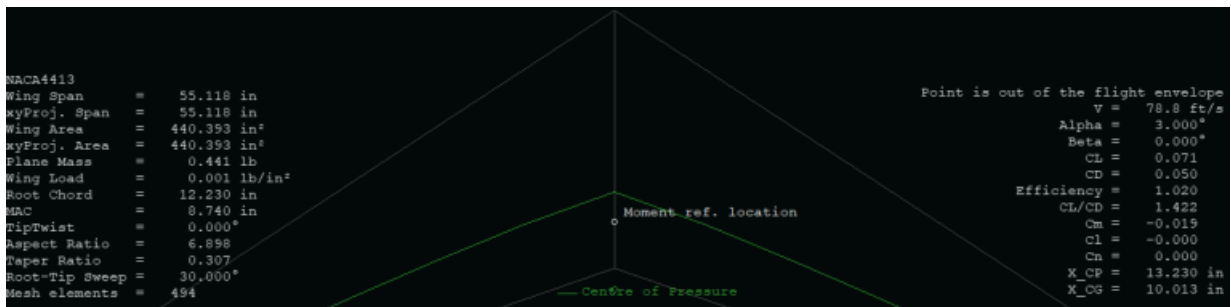


Figure 3.31: NACA 4413 Pitching Moment at Low Angles of Attack



Figure 3.32: NACA 4413 Pitching Moment at High Angles of Attack

The center of pressure line as shown above being towards the trailing edge of the wing model at 3 degrees, composing of a backward lift section that is close to zero that would cause a further upstream moment distribution as the coefficient of lift increases at angle of attack of 5 degrees or higher. At higher angles, the center of pressure line is furthest towards leading edge as represented at 9.4 degrees.

3.3.7. NACA 6410

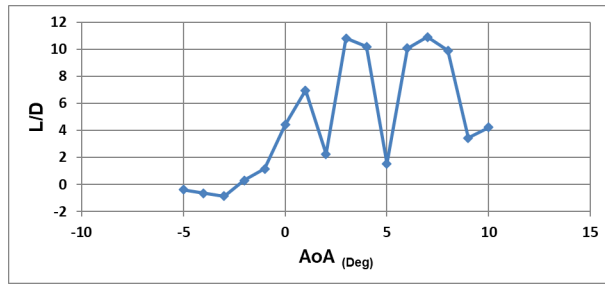


Figure 3.33: L/D vs. AoA with NACA 6410 Wing

The max L/D of the AL 37 with the NACA 6410 wing is about 11 degrees at an angle of attack of 7.5 degrees. From the airfoils tested, this is stable. However, this does not have a straight pattern when it comes to L/D vs. AoA. This may be due to the model of the wing.

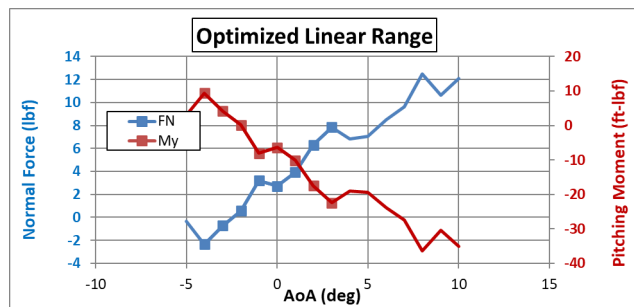


Figure 3.34: Optimized Linear Range with NACA 6410 Wing

The optimized angle of attack of the aircraft is calculated where the normal force and pitching moment intersect. For the NACA 6410, the optimized AoA is 1 degree. Like the L/D graph however, the curve is not straight, instead being erratic.

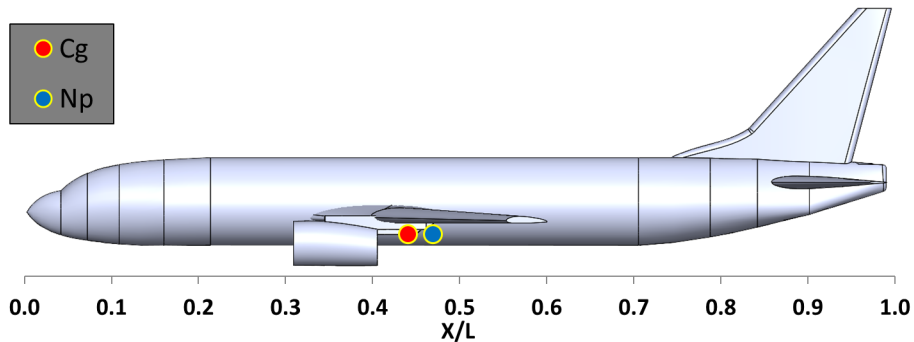


Figure 3.35: CG and NP Placement with NACA 6410 Wing

The neutral point of the AL 37 is important in order to define the stability of the aircraft. The center of gravity of the aircraft is 2.9167 from the nose of the aircraft. The neutral point 3.1045 from the nose. The static margin is 28.61%

3.3.8. Clark Y

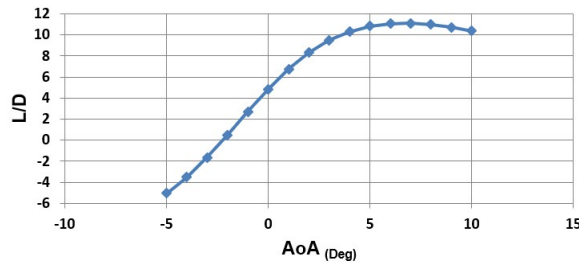


Figure 3.36: L/D vs. AoA with Clark Y Wing

The max L/D of the AL-37 with the Clark Y wing is 11.107 at an angle of attack of 7 degrees. From the airfoils tested this is the highest L/D value. It is also important to note that over a angle of attack range of 0 degrees to 5 degrees the Clark Y also has the highest L/D. As we are attempting to maximize the aerodynamic performance of the AL-37, this optimized L/D is intriguing.

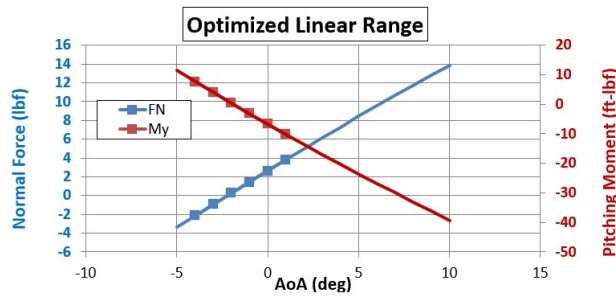


Figure 3.37: Optimized Linear Range with Clark Y Wing

The optimized angle of attack of the aircraft is calculated by finding where the normal force and Pitching Moment intersect. For the Clark Y, the optimized linear range provides at an angle of attack of 2 degree.

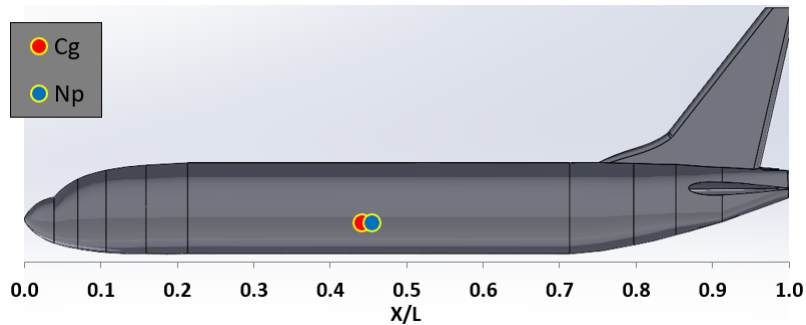


Figure 3.38: CG and NP Placement with Clark Y Wing

The relationship between the center of gravity and the neutral point of the aircraft is extremely important in order to define the stability. The center of gravity of the aircraft is 2.917 ft from the nose while the neutral point is 3.998 ft from the nose. This leads to a static margin of 12.32%.

4

Results

The team looked over initial results from the airfoil analysis to determine any outliers to remove or heavily consider. The NACA 6410 was removed from consideration as though it was statically stable, the lift-over-drag and optimized linear range graphs gave more erratic results compared to the others, and if the AoA vs. L/D graph is accurate, the aircraft would temporarily stall at 5 degrees, then approach stall again around 9 degrees. For this reason, the airfoil was removed from consideration.

The NACA 1412 and NACA 2211 were also eliminated, as those two airfoils yielded statically unstable results. This left the NACA 2412, NACA 3510, NACA 4413, YS-930, and Clark-Y airfoils. Using MATLAB, plots of the lift, drag, pitching moment, L/D, and optimized linear range for the four airfoils, as well as the AL-37 airfoil, were created, as shown in the figures below.

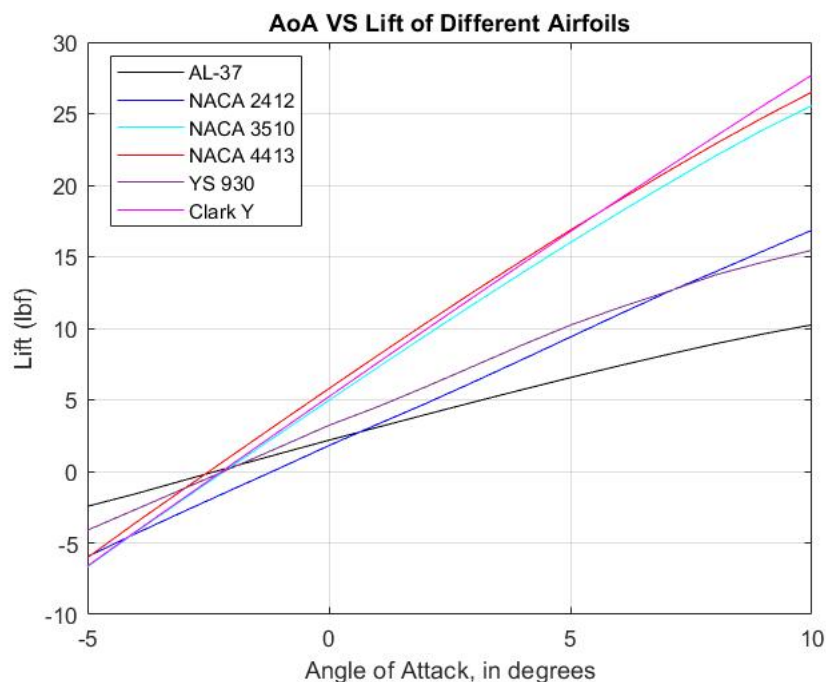


Figure 4.1: AoA vs. Lift for All Candidate Airfoils

The AoA vs. Lift shows that the Clark Y and NACA 3510 provide the best lift at steady-level and higher angles of attack. The Clark Y provides slightly more lift at roughly 28 lbf at 10 degrees, compared to the NACA 3510 at 25 lbf. The NACA 2412 and YS-930 trail behind. The AL-37 airfoil has the least lift loss at angles of attack below -3 degrees, but it generates significantly less lift compared to the other airfoils.

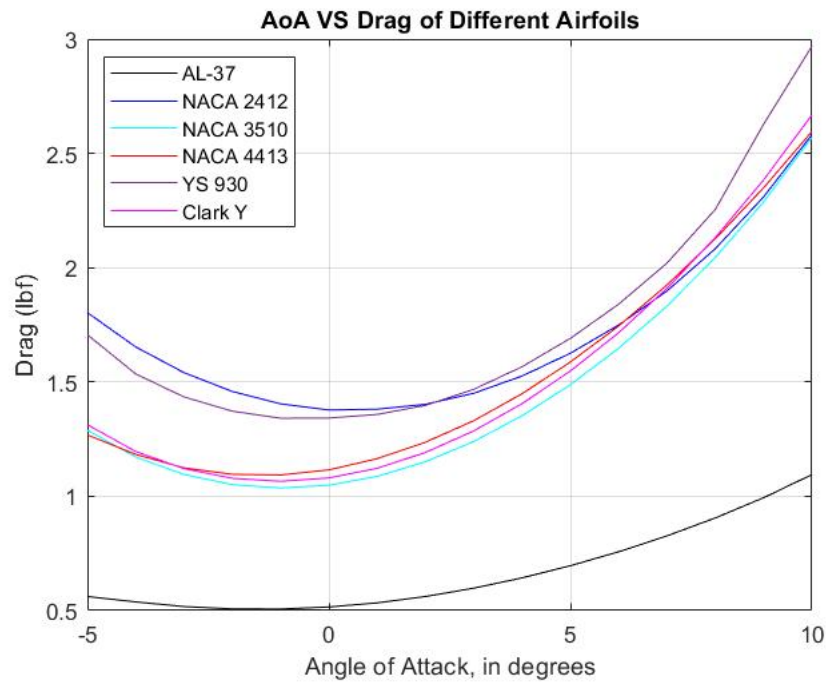


Figure 4.2: AoA vs. Drag for All Candidate Airfoils

The AL-37 airfoil generates very little drag. The NACA 3510 and Clark Y generate the least afterward, at roughly 1.1 lbf at steady-level flight. The NACA 2412 generates the most drag up until roughly 2 degrees AoA, before being overtaken by the YS-930.

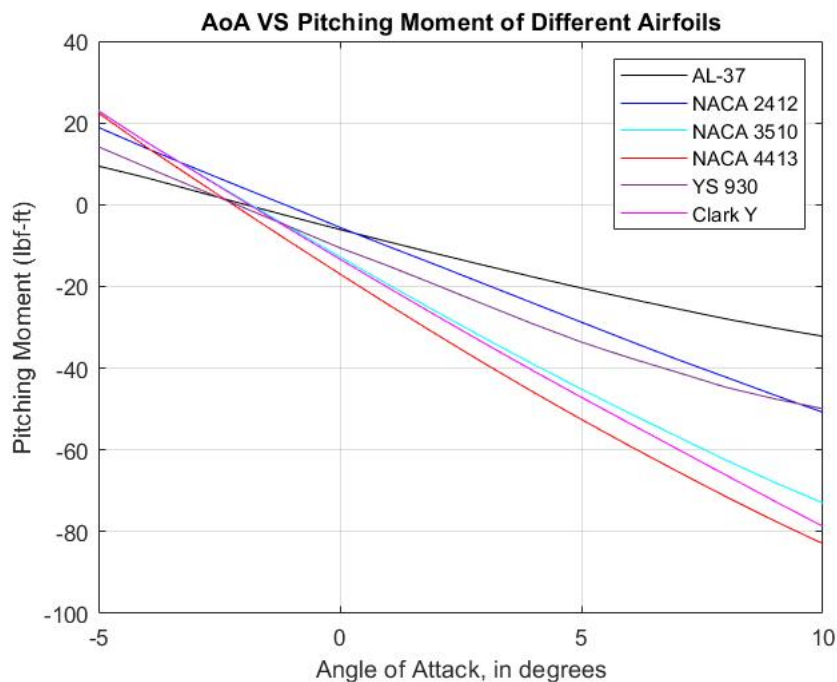


Figure 4.3: AoA vs. Pitching Moment for All Candidate Airfoils

All airfoils feature a downward linear curve. The AL-37 and NACA 2412 generate the least pitching moment at steady-level flight, both around -7 lbf-ft. The Clark Y and NACA 3510 generate the most, and have a sharper decline compared to the other airfoils, generating up to -70 to -80 lbf-ft at 10

degrees.

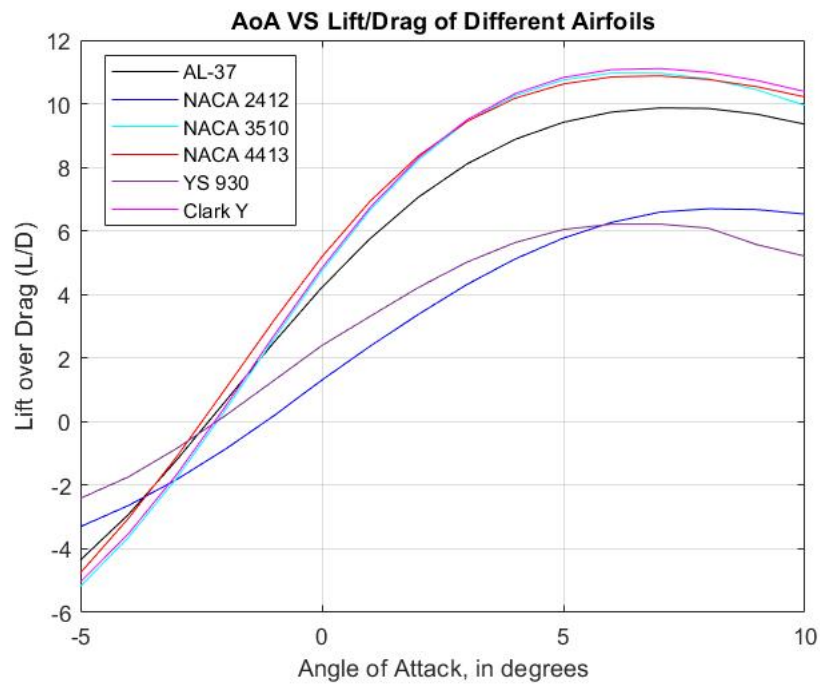


Figure 4.4: AoA vs. L/D for All Candidate Airfoils

The Clark Y and NACA 3510 feature the greatest lift-to-drag ratio. The maximum value is at 7 degrees, with both wings generating a lift 11 times the amount of drag being generated. The YS-930 and NACA 2412 both fall below the AL-37's curve past -4 degrees.

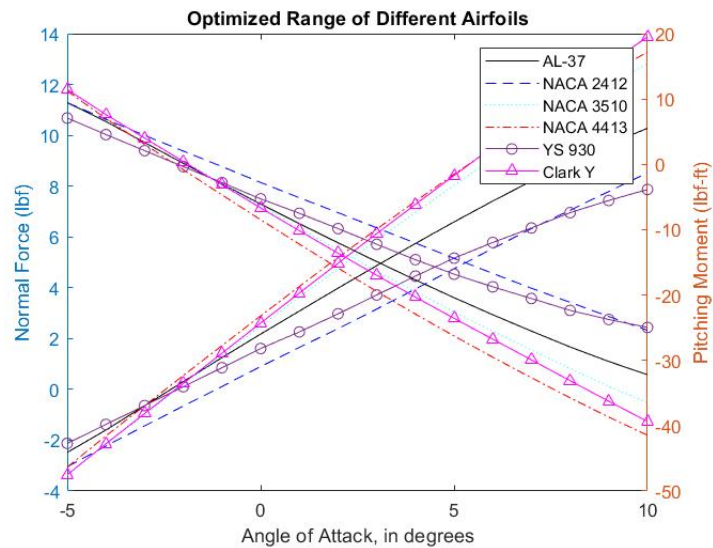


Figure 4.5: Optimized Linear Range for All Candidate Airfoils

The Clark Y and NACA 3510's optimized ranges both cross around 2 degrees, making them the most optimized for closer to steady-level flight. The AL-37 airfoil is optimized at 3 degrees, followed by the YS-930 and NACA 2412 closer to 5 degrees.

From the data and graphs, the Clark Y and NACA 3510 provide the best lift and lift-over-drag results, as well as falling in the preferred static margin range. The Clark Y has slightly better performance, but is 0.5% less stable than the NACA 3510. As both wings performance near-identically, the team determined that the extra stability would be a higher priority to get slightly closer to the AL-37 airfoil's static margin. As a result, the NACA 3510 was chosen to be the next airfoil for the truss-braced wing. The full data results for each wing that underwent CFD analysis are listed in Tables 4.1 and 4.2.

	AL-37	NACA 3510	Clark Y	NACA 2412	NACA 4413	YS-930
Static Margin	25%	13%	12.5%	3.71%	53.97%	53.1%
Maximum L/D AoA	7	7	7	8	7	7
Maximum L/D	9.86	11.0	11.1	6.69	10.9	6.21
Negative Cm Plot	Yes	Yes	Yes	Yes	Yes	Yes
Lift at 10 AoA	10.2	25.6	27.7	16.9	21.42	15.5
Steady-Level Moment	-2 lbf-ft	-2 lbf-ft	-2 lbf-ft	-1 lbf-ft	-1.06 lbf-ft	-2 lbf-ft
Steady-Level Lift	2.17 lbf	4.97 lbf	5.22 lbf	1.80 lbf	5.78 lbf	3.21 lbf
Steady-Level Drag	0.52 lbf	1.04 lbf	1.08 lbf	1.38 lbf	1.12 lbf	1.34 lbf
Steady-Level L/D	4.22	4.74	4.83	1.31	5.19	2.40

Table 4.1: Candidate Airfoil CFD Data

	NACA 1412	NACA 2211	NACA 6410
Static Margin	-38%	-29%	28%
Maximum L/D AoA	8	8	7
Maximum L/D	10.35	9.58	10.9
Negative Cm Plot	Yes	Yes	Yes
Lift at 10 AoA	22.5	20.0	23.6
Steady-Level Moment	-2.89 lbf-ft	-3.65 lbf-ft	-12.8
Steady-Level Lift	1.27 lbf	1.80 lbf	5.43 lbf
Steady-Level Drag	0.99 lbf	0.94 lbf	1.23 lbf
Steady-Level L/D	1.90	1.29	4.41

Table 4.2: Eliminated Airfoil CFD Data

5

Conclusion

Overall, the results of the airfoils were sufficient. However, the NACA 4413 airfoil that we chose has close to zero coefficient of lift to an angle of attack at 3 degrees at the speeds our aircraft would be traveling at. This would be more suited to larger-scale aircraft. We decided to abandon that airfoil as it was not going to help us with our data. The NACA 1412 and NACA 2211 were also found to be unstable after analysis, so they were abandoned as well. Otherwise, all other airfoils are stable on the AL-37.

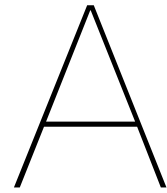
We brought our choice of airfoils down to the Clark Y and NACA 3510 airfoils and they have the best and greatest lift-to-drag ratio. They are also both well-optimized for steady-level flight. Both wings provide nearly the same performance. However, we sided with the NACA 3510 as this provides extra stability for our truss-braced wing for the AL-37.

6

Bibliography

- [1] T. Grager, "CFD-Data-CG-Static-Margin.xlsm" Aug. 20, 2022. [Accessed Sep. 22, 2022]
- [2] D. Faconti, "PlotJuggler," Apr. 24, 2022. [Online] Available: <https://github.com/facontidavide/PlotJuggler>. [Accessed Apr. 26, 2022]
- [3] AirfoilTools, "CLARK Y AIRFOIL (clarky-il)." [Online] Available: <http://airfoiltools.com/airfoil/details?airfoil=clarky-il>
- [4] AirfoilTools, "NACA-1412 AIRFOIL (naca1412-il)." [Online] Available: <http://airfoiltools.com/airfoil/details?airfoil=naca1412-il>
- [5] AirfoilTools, "NACA-2412 AIRFOIL (naca2412-il)." [Online] Available: <http://airfoiltools.com/airfoil/details?airfoil=naca2412-il>
- [6] AirfoilTools, "YS-930 AIRFOIL (ys930-il)." [Online] Available: <http://airfoiltools.com/airfoil/details?airfoil=ys930-il>

Special thanks to Dr. Stephen Holland, Dr. Bong Wie, Professor Travis Grager, and Dr. Dayal Vinay for their assistance and insight during the analysis process.



Data Graphing Utility Source Code

```
1
2 close all;
3 clearvars -except csv;
4
5 %importing the data from PlogJuggler
6 %recomend running once then commenting out this line as it takes minutes to
7 %run otherwise
8 csv = importdata("DataFlightOne.csv");
9
10
11 %conversion factors
12 mm2ft = 1/305; %305 mm is about 1 ft
13 mps2mph = 2.237; %1 m/s is about 2.237 mph
14 %end
15
16 %main code
17 altGps = vsTime(csv,"sensor_gps/alt"); %constucting [time; altitude]
18 altGps = [altGps(1,:)- altGps(1,1); altGps(2,:).*mm2ft - altGps(2,1)*mm2ft]; %normalising at
    runway and converting m/s to fps
19 graph(altGps, 'Time (s)', "Altiude (Ft)") %graphing
20 aveAltGps = mean(altGps(2,182:302)); %ave over t=180 to t=300
21
22 discharge = vsTime(csv,"mah_per_sec"); %constucting [time; discharge rate]
23 graph(discharge, 'Time (s)', 'Discharge rate (mAH/s)') %graphing
24 aveDischarge = mean(discharge(2,686:1436)); %averaging over t=150 to t=300
25
26 velGps = vsTime(csv, "vehicle_gps_position/vel_m_s"); %constucting [time; ground speed]
27 velGps = [velGps(1,:); velGps(2,:).*mps2mph];%converting m/s to fps
28 graph(velGps, 'Time (s)', "Ground Velocity (mph)") %graphing
29 aveVelGps = mean(velGps(2,66:627));%ave over t=45 to t=325
30
31 totalDischarge = vsTime(csv,'battery_status/discharged_mah'); %constucting [time; mah used]
32 graph(totalDischarge, 'Time (s)', "Amount Discharged (mAH)") %graphing
33 %end
34
35
36 %Functions
37
38 %returns horizontal vector from one column of data out of the larger csv
39 %DOES NOT REMOVE ANY NaN DATA CELLS
40 %csv is the structure that got imported from PlotJuggler
41 %exactTag is the label that the pixhawk assigns to the data in intrest
42 function dataOut = rawData(csv, exactTag)
43     dataOut = csv.data(:,find(strcmp(csv.colheaders, exactTag)))';
44 end
45
46 %returns a maxtrix of [time; data]
47 %removes any NaN data as to prevent issues from them
48 %csv is the structure that got imported from PlotJuggler
49 %exactTag is the label that the pixhawk assigns to the data in intrest
```

```
50 function dataOut = vsTime(csv, exactTag)
51     time = rawData(csv, '__time');
52     data = rawData(csv, exactTag);
53     dataOut = rmmissing([time;data],2);
54 end
55
56 %graphs the data
57 %data must be in the order of [X values; Y values]
58 %i is used to keep each plot seperated and in their own window
59 %labelX and labelY are passed to their labeling commands
60 function graph(data, labelX, labelY)
61     figure
62     plot(data(1,:),data(2,:))
63     xlabel(labelX)
64     ylabel(labelY)
65 end
```

B

Post-CFD MATLAB Analysis Code

```
1 % Boeing Experimental Flight
2 % Star-CCM CFD Analysis
3
4 clear all
5 %% Table Imports
6
7 ys = 'CFD-Data-Static-Margin-YS930 with updated CG.xlsm';
8 xlRange = 'C17:R32';
9 Ys930 = xlsread(ys,xlRange);
10
11 n6410 = 'CG-Static-Margin-NACA6410.xlsm';
12 NACA6410 = xlsread(n6410,xlRange);
13
14 n3510 = 'CFD-Data-NACA_3510.xlsm';
15 NACA3510 = xlsread(n3510,xlRange);
16
17 clark = 'CFD-Data-Clark-Y.xlsm';
18 ClarkY = xlsread(clark,xlRange);
19
20 n2211 = 'CFD-Data-NACA_2211.xlsm';
21 NACA2211 = xlsread(n2211,xlRange);
22
23 n1412 = 'CFD-Data-NACA1412.xlsm';
24 NACA1412 = xlsread(n1412,xlRange);
25
26 n2412 = 'CFD-Data-Static-Margin-NACA2412.xlsm';
27 NACA2412 = xlsread(n2412,xlRange);
28
29 n4413 = 'CFD-Data-Static-Margin-NACA4413';
30 NACA4413 = xlsread(n4413,xlRange);
31
32 A1 = 'CFD-Data-AL37_V2.xlsm';
33 AL37 = xlsread(A1,xlRange);
34
35 %% AoA VS L/D Plot
36
37 figure(1)
38 plot(AL37(:,1),AL37(:,16),'k')
39 hold on
40 % plot(NACA1412(:,1),NACA1412(:,16),'r')
41 % plot(NACA2211(:,1),NACA2211(:,16),'g')
42 plot(NACA2412(:,1),NACA2412(:,16),'b')
43 plot(NACA3510(:,1),NACA3510(:,16),'c')
44 % plot(NACA6410(:,1),NACA6410(:,16),'y')
45 plot(NACA4413(:,1),NACA4413(:,16),'r')
46 plot(Ys930(:,1),Ys930(:,16),'Color','#7E2F8E')
47 plot(ClarkY(:,1),ClarkY(:,16),'m')
48 xlabel('Angle of Attack, in degrees')
49 ylabel('Lift over Drag (L/D)')
50 title('AoA VS Lift/Drag of Different Airfoils')
```

```

51 legend('AL-37','NACA 2412','NACA 3510','NACA 4413','YS 930','Clark Y')
52 grid on
53
54 %% AoA VS Lift Plot
55
56 figure(2)
57 plot(AL37(:,1),AL37(:,9),'k')
58 hold on
59 plot(NACA2412(:,1),NACA2412(:,9),'b')
60 plot(NACA3510(:,1),NACA3510(:,9),'c')
61 plot(NACA4413(:,1),NACA4413(:,9),'r')
62 plot(Ys930(:,1),Ys930(:,9),'Color','#7E2F8E')
63 plot(ClarkY(:,1),ClarkY(:,9),'m')
64 xlabel('Angle of Attack, in degrees')
65 ylabel('Lift (lbf)')
66 title('AoA VS Lift of Different Airfoils')
67 legend('AL-37','NACA 2412','NACA 3510','NACA 4413','YS 930','Clark Y')
68 grid on
69
70 %% AoA VS Drag Plot
71
72 figure(3)
73 plot(AL37(:,1),AL37(:,10),'k')
74 hold on
75 plot(NACA2412(:,1),NACA2412(:,10),'b')
76 plot(NACA3510(:,1),NACA3510(:,10),'c')
77 plot(NACA4413(:,1),NACA4413(:,10),'r')
78 plot(Ys930(:,1),Ys930(:,10),'Color','#7E2F8E')
79 plot(ClarkY(:,1),ClarkY(:,10),'m')
80 xlabel('Angle of Attack, in degrees')
81 ylabel('Drag (lbf)')
82 title('AoA VS Drag of Different Airfoils')
83 legend('AL-37','NACA 2412','NACA 3510','NACA 4413','YS 930','Clark Y')
84 grid on
85
86 %% AoA VS Pitching Moment Plot
87
88 figure(4)
89 plot(AL37(:,1),AL37(:,11),'k')
90 hold on
91 plot(NACA2412(:,1),NACA2412(:,11),'b')
92 plot(NACA3510(:,1),NACA3510(:,11),'c')
93 plot(NACA4413(:,1),NACA4413(:,11),'r')
94 plot(Ys930(:,1),Ys930(:,11),'Color','#7E2F8E')
95 plot(ClarkY(:,1),ClarkY(:,11),'m')
96 xlabel('Angle of Attack, in degrees')
97 ylabel('Pitching Moment (lbf-ft)')
98 title('AoA VS Pitching Moment of Different Airfoils')
99 legend('AL-37','NACA 2412','NACA 3510','NACA 4413','YS 930','Clark Y')
100 grid on
101
102 %% Optimize Range Plot
103
104 figure(5)
105 yyaxis left
106 plot(AL37(:,1),AL37(:,4),'k')
107 hold on
108 plot(NACA2412(:,1),NACA2412(:,4),'b')
109 plot(NACA3510(:,1),NACA3510(:,4),'c')
110 plot(NACA4413(:,1),NACA4413(:,4),'r')
111 plot(Ys930(:,1),Ys930(:,4),'Color','#7E2F8E')
112 plot(ClarkY(:,1),ClarkY(:,4),'m')
113 xlabel('Angle of Attack, in degrees')
114 ylabel('Normal Force (lbf)')
115 title('Optimized Range of Different Airfoils')
116 legend('AL-37','NACA 2412','NACA 3510','NACA 4413','YS 930','Clark Y')
117
118 yyaxis right
119 plot(AL37(:,1),AL37(:,5),'k')
120 plot(NACA2412(:,1),NACA2412(:,5),'b')
121 plot(NACA3510(:,1),NACA3510(:,5),'c')

```

```
122 plot(NACA4413(:,1),NACA4413(:,5),'r')
123 plot(Ys930(:,1),Ys930(:,5),'Color','#7E2F8E')
124 plot(ClarkY(:,1),ClarkY(:,5),'m')
125 ylabel('Pitching Moment (lbf-ft)')
126 legend('AL-37','NACA 2412','NACA 3510','NACA 4413','YS 930','Clark Y')
127
128 hold off
```